Acta Biochim Biophys Sin, 2016, 48(5), 430–436
doi: 10.1093/abbs/gmw020
Original Article

Original Article

Downregulation of myosin VI reduced cell growth and increased apoptosis in human colorectal cancer

Weiqiang You[1,†], Gewen Tan[1,†], Nengquan Sheng[1], Jianfeng Gong[1], Jun Yan[1], Di Chen[2], Huizhen Zhang[3], and Zhigang Wang[1,*]

[1]Department of General Surgery, Shanghai Jiao Tong University Affiliated Sixth People's Hospital, Shanghai 200233, China, [2]National Key Laboratory of Science and Technology on Nano/Micro Fabrication Technology, Research Institute Micro/Nano Science and Technology, Shanghai Jiao Tong University, Shanghai 200240, China, and [3]Department of Pathology, Shanghai Jiao Tong University Affiliated Sixth People's Hospital, Shanghai 200233, China

[†]These authors contributed equally to this work.
*Correspondence address. Tel/Fax: +86-21-24058549; E-mail: surlab@hotmail.com

Received 31 December 2015; Accepted 25 February 2016

Abstract

Colorectal cancer (CRC) is the third most commonly diagnosed cancer worldwide, with the mortality increasing steadily over the last decade. *Myosin VI (MYO6)* expression is found to be elevated in some types of human carcinoma cell types, suggesting that it may be a sensitive biomarker for the diagnosis and follow-up. In this study, we first used the Oncomine database to explore the expression of *MYO6* in CRC tissues, and then constructed a plasmid of RNA interference targeting MYO6 gene. After transfection of lentivirus targeting *MYO6* into SW1116 cells, cell viability and proliferation were measured with 3-(4,5-Dimethylthiazol-2-yl)-2,5-diphenyltetrazolium bromide and colony formation assay. Cell cycle distribution was assayed by flow cytometry and apoptosis was evaluated by Annexin V. *MYO6* expression was detected by quantitative real-time polymerase chain reaction and western blot analysis. It was found that MYO6 mRNA was upregulated in CRC tissues using data mining of public Oncomine microarray datasets. Depletion of *MYO6* significantly inhibited cell proliferation and colony formation. In addition, knockdown of *MYO6* slightly arrested cell cycle in G0/G1 phase, but remarkably increased the proportion of the sub-G1 phase of cell with the increase of apoptotic cells. These results suggest that *MYO6* may promote cell growth and may be used as a potential target for anticancer therapy of CRC.

Key words: colorectal cancer, MYO6, shRNA, proliferation, apoptosis

Introduction

Despite a remarkable decline in mortality over the past decade, colorectal cancer (CRC) remains one of the most common cancers worldwide [1]. It is the third most common cancer and the third leading cause of cancer-related death in men and women, involving 136,830 diagnosed patients and 50,310 deaths in the USA in 2014 [2]. The incidence and mortality of CRC in China are lower than those in western countries, though they have been gradually increasing in recent years [3,4]. Even after excision, the 2-year recurrence rate is as high as 75%, and the 5-year survival rate is only 26.8% [5,6]. Therefore, developing new therapeutic drugs for CRC remains a challenge. Colorectal carcinogenesis involves multistep molecular processes with sequential activation of oncogenes and inactivation of tumor suppressor genes. More and more oncogenes and tumor suppressor genes have been identified during the course of CRC in recent years.

Most of myosins in the myosin superfamily are defined as actin-based motor molecules that mainly participate in cellular processes based on actin and move on the actin filaments driven by adenosine

triphosphate (ATP) hydrolysis [7,8]. Unconventional myosins have been implicated in F-actin-mediated cellular functions such as cell motility, vesicular trafficking, as well as intracellular transport of macromolecules. And members of myosins also play an important role in signal transduction [9–11]. *Myosin VI (MYO6)* is a unique member of the unconventional myosin family, and a reverse-direction motor protein that moves toward the minus-end of actin filaments [12]. The MYO6 protein has a motor domain containing an ATP-actin-binding site and a globular tail that interacts with other proteins. An interesting link between *MYO6* and human cancers has been described in previous studies. Yoshida *et al*. [13] found that there was a positive correlation between aggressive ovarian cancer and *MYO6* overexpression. Some recent studies demonstrated that *MYO6* acted as a novel oncogene in human prostate cancer [14–17]. It was found that knockdown of *MYO6* gene by siRNA inhibited prostate tumor growth and metastasis by decreasing the secretion of prostate specific antigen and the vascular endothelial growth factor. Similar results were also obtained in human lung cancer cells [18].

However, no study on *MYO6* expression in CRC has been reported so far. In this study, we first observed the overexpression of *MYO6* in CRC by the data mining from the public Oncomine microarray database. To investigate the role of *MYO6* in CRC cells, we silenced *MYO6* gene in CRC cell line SW1116 using lentivirus-mediated gene delivery method, and analyzed the biological function after the knockdown of *MYO6 in vitro*. Our results suggest that inhibition of *MYO6* by siRNA might be a potential therapeutic strategy for the treatment of CRC.

Materials and Methods

Oncomine analysis

To determine the expression level of *MYO6* in CRC, five datasets (Sabates-Bellver Colon, Skrzypczak Colorectal, Hong Colorectal, Kaiser Colon, and TCGA Colorectal) in Oncomine database (https://www.oncomine.org) were selected [19]. The expression difference of *MYO6* gene was compared between the CRC tissues and normal tissues. The log-transformed and normalized expression values of *MYO6* were extracted, analyzed, and read from the bar chart.

Cell lines and cell culture

Human colon cancer SW1116 cells (Cat No. TCHu 174) and human embryonic kidney 293T cells (Cat No. GNHu17) were obtained from the Cell Bank of Chinese Academy of Science (Shanghai, China). SW1116 and 293T cells were maintained in Dulbecco's modified Eagle's medium (Hyclone, Logan, USA) supplemented with 10% fetal bovine serum (FBS; Biological Industries, Cromwell, USA), respectively. Both cell lines were cultured at 37°C in a 5% CO_2 humidified incubator.

Lentivirus-mediated short hairpin RNA knockdown of *MYO6* expression

The short hairpin RNA (shRNA) sequences specifically targeting the nucleotides of human *MYO6* gene (NM_004999) were designed through Sigma-Aldrich web-based tool (http://www.sigmaaldrich.com/). BLAST homology search was used to verify the 100% similarity of oligonucleotides and the effective cDNA sequences of *MYO6* genes from various species. The non-silencing shRNA was used as a control that has no homology with any gene in human as determined by screening with NCBI RefSeq. The shRNA sequences were as follows—MYO6 shRNA (S1): 5′-GTGAATCCAGAGATAAGTTTACT CGAGTAAACTTATCTCTGGATTCACTTTTT-3′, MYO6 shRNA (S2): 5′-CCAGATTTAACCATTCCATAACTCGAGTTATGGAAT GGTTAAATCTGGTTTTTT-3′ and the negative control shRNA was 5′-GCGGAGGGTTTGAAAGAATATCTCGAGATATTCTTT CAAACCCTCCGCTTTTTT-3′. The double-stranded DNA fragments were formed in the annealing reaction system. The pFH-L vector (Shanghai Hollybio, Shanghai, China) was linearized by *Eco*RI and *Bam*HI restriction enzyme digestion. Pure linearized vector fragments and double-stranded DNA fragments were collected and combined together during a 16 h reaction. Each DNA was used to transform the *Escherichia coli* strain DH5α and purified with a plasmid purification kit (Qiagen, Valencia, USA). The ligation product was confirmed by polymerase chain reaction (PCR) and sequencing. The generated plasmids were named as pFH-Lv-shMYO6 (S1), pFH-Lv-shMYO6 (S2), or Lv-shCon. Recombinant lentiviral vectors and packaging pHelper plasmids (pVSVG-I and pCMVΔR8.92) (Shanghai Hollybio) were cotransfected into 293T cells. Supernatants containing lentivirus expressing shMYO6(S1), shMYO6(S2), or control shRNA (shCon) were harvested 48 h after transfection. Then, the lentiviruses were purified via ultracentrifugation, and the viral titer was determined by counting the green fluorescent protein (GFP)-positive cells. Viral titer was determined by the method of end point dilution through counting the numbers of infected GFP-positive cells at ×100 magnification under a fluorescence microscope (Olympus, Tokyo, Japan) 3 days after infection to 293T cells. Titer (IU/ml) = the numbers of green fluorescent cells × dilution factor/volume of virus solution [20]. For lentivirus infection, SW1116 cells (40,000 cells/well) were seeded in six-well plates and transduced with shMYO6(S1), shMYO6(S2), or shCon at a multiplicity of infection of 25. Infection efficiency was determined through counting the GFP-positive cells under a fluorescence microscope 72 h after infection, and the knockdown efficiency of *MYO6* was evaluated by quantitative real-time polymerase chain reaction (qRT-PCR) and western blot analysis.

Reverse transcription-PCR and quantitative real-time PCR

After 5 days of lentivirus infection, total cellular RNA was extracted using Trizol reagent (Invitrogen, Carlsbad, USA). RNA quantity and quality were determined by spectrophotometry and agarose gel electrophoresis, respectively. Extracted total RNA samples (1 μg) was reverse transcribed into cDNA with oligod(T) primers according to the manufacturer's protocol for reverse transcription PCR (Promega, Fitchburg, USA). qRT-PCR was carried out by using the GXD kit iq-SYBR Green (BioRad, Hercules, USA) according to the manufacturer's instructions with the CFX96 Touch™ Real-Time PCR Detection System (BioRad). Primer sets used were as follows: for *β-actin*, 5′-GTGGACATCCGCAAAGAC-3′ (forward), 5′-AAA GGGTGTAACGCAACTA-3′ (reverse) and for *MYO6*, 5′-AATCAC TGGCTCACATGCAG-3′ (forward), 5′-AATGCGAGGTTTGTGTC TCC-3′ (reverse). The cycling conditions were as follows: initial denaturation 95°C for 60 s, 95°C for 5 s, 60°C for 20 s, 40 cycles. Data analysis was performed using the $2^{-\Delta\Delta C_t}$ method.

Western blot analysis

After 7 days of lentivirus infection, cells were harvested and lysed in ice-cold lysis buffer [50 mM Tris, 2% sodium dodecyl sulphate (SDS), 5% glycerinum, 100 mM NaCl, 1 mM ethylenediaminetetraacetic acid, pH 6.8]. Total protein concentrations of the lysate were determined using BCA Protein Assay Kit (Pierce Biotechnology, Rockford, USA). A total of 30 μg protein in each lane was electrophoresed on 10% SDS-polyacrylamide gel electrophoresis gel and transferred to

polyvinylidene fluoride membrane (BioRad), and incubated with rabbit anti-MYO6 (Sigma, St Louis, USA) and rabbit anti-glyceraldehyde-3-phosphate dehydrogenase (GAPDH) (1 : 40,000; Proteintech, Rosemont, USA) overnight at 4°C. Membranes were then incubated with horseradish peroxidase-conjugated goat anti-rabbit immunoglobulin G secondary antibody (1 : 5000; Santa Cruz Biotechnology, Santa Cruz, USA). Signals were detected using the ECL-PLUS Kit (Amersham, Piscataway, USA) according to the manufacturer's protocol. GAPDH was used as the internal standard.

MTT assay

The effect of *MYO6* on cell viability was analyzed using the 3-(4,5-Dimethylthiazol-2-yl)-2,5-diphenyltetrazolium bromide (MTT) assay based on growth curves of SW1116 cells *in vitro*. Briefly, cells were seeded in 96-well plates at a concentration of 2500 cells/well in 200 μl/well after 3 days of lentivirus infection. Cells were then further cultured in this manner for 1–5 days. Four hours before the termination of culture, MTT (5 mg/ml; Sigma) was added at a volume of 20 μl/well. Afterward, the acidic isopropanol (0.01 M HCl, 10% SDS and 5% isopropanol) was added at a volume of 100 μl/well and incubated overnight at 37°C. The absorbance at 595 nm of each well was determined using the Epoch Microplate Spectrophotometer (BioTek, Shoreline, USA).

Colony formation assay

After 3 days of lentivirus infection, SW1116 cells (500 cells/well) were seeded in 6-well plates and incubated for 10 days to form normal colonies. The media were replaced every 3 days. Then the cells were fixed with paraformaldehyde for 30 min at room temperature. The fixed cells were washed twice with phosphate buffered saline (PBS), stained with 1% crystal violet (Beyotime, Shanghai, China) for 10 min, washed with ddH_2O and air dried. The total number of colonies that contain >50 cells was counted under a light microscope. Image analysis was conducted using Image-Pro Plus 6.0 software (Media Cybernetics, Rockville, USA).

Cell cycle analysis

After 4 days of lentivirus infection, SW1116 cells were seeded in 6-cm dishes at a density of 80,000 cells/dish and cultured for 40 h. Cells were then released by digestion with trypsin and harvested. After centrifugation, the cell pellet was washed twice with precooled PBS and fixed with precooled 70% ethanol overnight at 4°C. Then cells were washed twice with precooled PBS and resuspended in PBS containing 10% FBS, filtered through a 400-mesh sieve, and stained with propidium iodide solution (PI, 50 μg/ml, 100 μg/ml RNase in PBS) at 37°C in the dark for 30 min. Finally, cells were analyzed for the cell cycle phase by FACScan (Beckman Coulter, Brea, USA). The percentages of cells at various phases of the cell cycle were analyzed using the ModFit (Verity Software House, Topsham, USA) software.

Apoptosis analysis

To determine the apoptosis of SW1116 cells, cells were subject to two different treatments [shCon and shMYO6(S2)]. Infected by lentivirus for 72h, thereafter, the cells were resuspended and reseeded in 6-cm dishes at a density of 80,000 cells/dish. After 24 h, the cells were collected, washed, and subjected to Annexin V-APC/7-AAD double staining according to the manufacture's instruction (KeyGEN Biotech, Nanjing, China). Flow cytometry analysis was performed on Cell Quest FACS system (BD Biosciences, San Jose, USA) to assess the apoptotic and viable cell fractions.

Statistical analysis

The results were expressed as the mean ± SD. Differences between the two groups were assessed using a two-tailed *t*-test. The $P < 0.05$ was defined as a significant difference. Statistical analysis was performed with GraphPad Prism 6 (GraphPad Software, Inc., San Diego, USA).

Results

MYO6 mRNA was overexpressed in CRC

By using the Oncomine database mining, we examined and analyzed the expression level of *MYO6* in CRC tissues. As shown in **Fig. 1**, all of the five datasets showed that MYO6 expression is significantly elevated in CRC compared with the normal tissues. Sabates-Bellver Colon dataset [21] showed *MYO6* expression in colon adenoma ($n = 25$), and rectal adenoma ($n = 7$) was higher than that in the normal tissues ($P = 8.52 \times 10^{-8}$ and $P = 3.62 \times 10^{-4}$, respectively) (**Fig. 1A**). It was also found that *MYO6* expression was significantly increased in Skrzypczak Colorectal dataset ($n = 45$, $P = 2.80 \times 10^{-6}$) (**Fig. 1B**) [22]. Another independent Hong Colorectal dataset [23] revealed that *MYO6* was upregulated in colorectal carcinoma ($n = 70$, $P = 0.004$) compared with normal colon tissues (**Fig. 1C**).

Similarly, TCGA Colorectal dataset (http://tcga-data.nci.nih.gov/tcga/) showed that the expression level of *MYO6* was also significantly higher in most CRC types than that in normal tissues (**Fig. 1D**), including cecum adenocarcinoma ($n = 22$, $P = 1.35 \times 10^{-5}$), colon adenocarcinoma ($n = 101$, $P = 1.45 \times 10^{-6}$), colon mucinous adenocarcinoma ($n = 22$, $P = 1.41 \times 10^{-5}$), rectal adenocarcinoma ($n = 60$, $P = 9.84 \times 10^{-10}$), and rectal mucinous adenocarcinoma ($n = 6$, $P = 0.004$), except rectosigmoid adenocarcinoma ($n = 3$) and rectosigmoid mucinous adenocarcinoma ($n = 1$) based on small sample numbers. Moreover, the result of Kaiser Colon dataset was similar to the above-mentioned findings, revealing that *MYO6* was significantly upregulated in rectal mucinous adenocarcinoma ($n = 4$) compared with normal colon tissues and slightly increased in other CRC types, including cecum adenocarcinoma ($n = 17$), colon adenocarcinoma ($n = 41$), colon mucinous adenocarcinoma ($n = 13$), colon signet ring cell adenocarcinoma ($n = 2$), colon small cell carcinoma ($n = 2$), rectal adenocarcinoma ($n = 8$), rectal mucinous adenocarcinoma ($n = 4$), rectosigmoid adenocarcinoma ($n = 10$), and rectosigmoid mucinous adenocarcinoma ($n = 2$), except rectal signet ring cell adenocarcinoma ($n = 1$) (**Fig. 1E**) [24]. These data suggest that *MYO6* plays a potential role in colon carcinogenesis.

MYO6 expression is reduced in lentivirus-transduced SW1116 cells

For functional study of *MYO6* in CRC cells, the *MYO6* gene was knocked down in SW1116 cells using a lentivirus-delivered shRNA specifically targeting human *MYO6* [shMYO6 (S1)/(S2)]. The infection efficacy was verified by the ratio of GFP-positive cells over 80% (**Fig. 2A**). To examine the knockdown efficacy, mRNA and protein in the SW1116 cells from different treatment groups were extracted for qRT-PCR and western blot analysis. As shown in **Fig. 2B**, MYO6 mRNA levels in groups transferred with shMYO6(S1) and shMYO6 (S2) were significantly lower than those in shCon group. The knockdown efficacy of MYO6 by shMYO6(S1) and shMYO6(S2) was 72% and 79.4%, respectively, suggesting that shRNA knockdown was specific and the loss-of-function outcome was not possibly caused by off-target effect. Western blot analysis also showed that MYO6 protein was reduced following *MYO6* knockdown (**Fig. 2C**). These

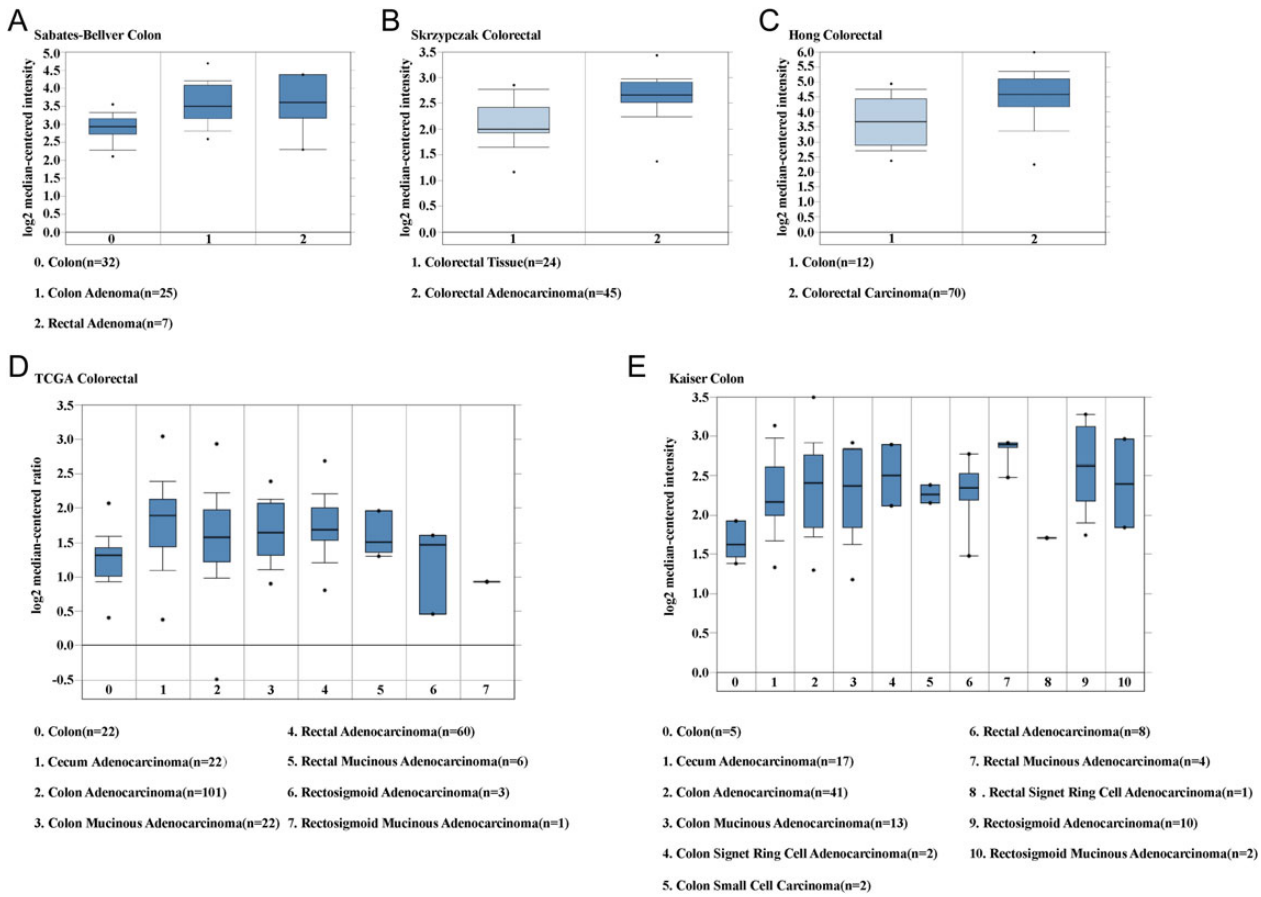

Figure 1. Analysis of MYO6 mRNA expression in human CRC using the Oncomine database (A) Detection of gene expression of MYO6 in normal, colon adenoma, and rectal adenoma tissues by the Sabates-Bellver Colon dataset. (B) Differences in MYO6 gene expression between normal and colorectal adenocarcinoma tissues were shown by the Skrzypczak Colorectal dataset. (C) MYO6 expression in the colon and colorectal carcinoma as shown by the Hong Colorectal dataset. (D,E) Differences in MYO6 expression between various CRC tissues and normal tissues were shown by the TCGA Colorectal and Kaiser Colon dataset. The total number of cases is shown under each graph. The *P* values were calculated by using two-tailed and Student's *t*-test. $^*P < 0.05$.

results suggested that MYO6 shRNA could significantly downregulate *MYO6* expression in SW1116 cells.

Knockdown of *MYO6* inhibits proliferation of SW1116 cells

MTT test showed that the OD value that represented the cell proliferation rate was increased from 1 to 3.2 in shCon group within 5 days after lentivirus transduction, while cell proliferation in shMYO6(S1) or shMYO6(S2) group was relatively slow, increasing from 1 to 2.6 in shMYO6(S1) group and from 1 to 1.2 in shMYO6(S2) group ($P < 0.001$; **Fig. 3A**) respectively, indicating that the proliferation of SW1116 cells was significantly impeded following *MYO6* knockdown.

Knockdown of *MYO6* restrains colony formation of SW1116 cells

In addition, the colony formation capacity of SW1116 cells was examined after *MYO6* knockdown. Representative photographs of the number of cells per colony and the number of colonies in per well were shown in **Fig. 3B**. Both cell and colony numbers were much smaller in shMYO6(S1) and shMYO6(S2) groups than those in shCon group. There were ~109 ± 4 colonies in shCon group vs. 78 ± 2 colonies in shMYO6(S1) group, indicating that the colony number was reduced by nearly 30% ($P < 0.005$; **Fig. 3C**). The colony number (22 ± 3) was reduced by ~80% in shMYO6(S2) group, compared with that in the shCon group ($P < 0.001$; **Fig. 3C**).

Knockdown of *MYO6* arrests cell cycle progression of SW1116 cells

To investigate whether cell cycle arrest contributed to cell growth inhibition, the cell cycle distribution in SW1116 cells was analyzed using fluorescence-activated cell sorting (FACS) (**Fig. 4A**). The results showed that knockdown of *MYO6* increased the percentage of G0/G1-phase cells in shMYO6(S2) group (54.50% ± 0.30% vs. 47.95% ± 0.13%; $P < 0.001$) and decreased the percentage in G2/M-phase cells (22.17% ± 0.52% vs. 28.59% ± 0.20%; $P < 0.001$) in comparison with the shCon group (**Fig. 4B**). Although the difference in G0/G1 and G2/M phases was small between shMYO6(S2) and shCon groups, it was worth noting that the shMYO6(S2) group exhibited a higher proportion of sub-G1 phase than the shCon group (3.20% ± 0.08% vs. 1.30% ± 0.12%; $P < 0.001$), suggesting that *MYO6* silencing induced cell apoptosis.

Knockdown of *MYO6* induces cell apoptosis in SW1116 cells

A distinct sub-G1 peak was observed in *MYO6* knockdown cells. To further confirm the effect of *MYO6* on cell apoptosis, Annexin V-APC/7-AAD double labeling of SW1116 cells was conducted to

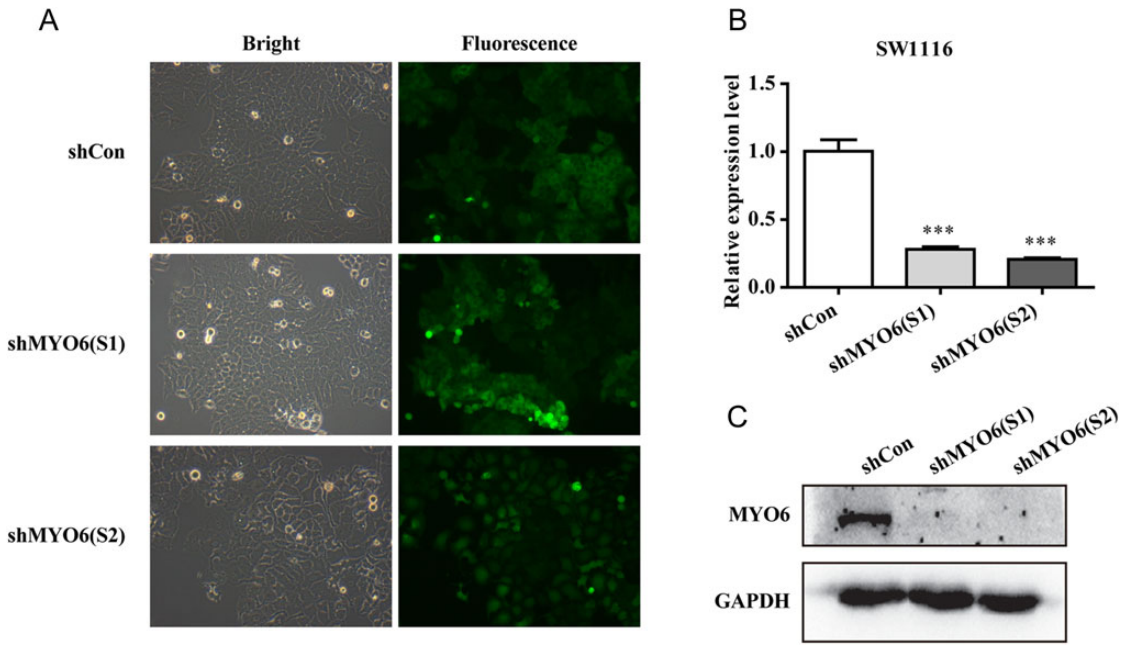

Figure 2. Lentivirus-mediated shRNA specifically reduced MYO6 expression in SW1116 cells (A) SW1116 cells under a ×100 magnification microscope and under inverted fluorescent microscope 96 h after lentivirus infection, where green fluorescent images show the successful infection of lentivirus expressing MYO6 shRNA (S1), MYO6 shRNA(S2), or Con shRNA. (B) qRT-PCR analysis of MYO6 mRNA levels in SW1116 cells after lentivirus infection. (C) Western blot analysis of MYO6 protein levels in SW1116 cells after lentivirus infection. ***$P < 0.001$.

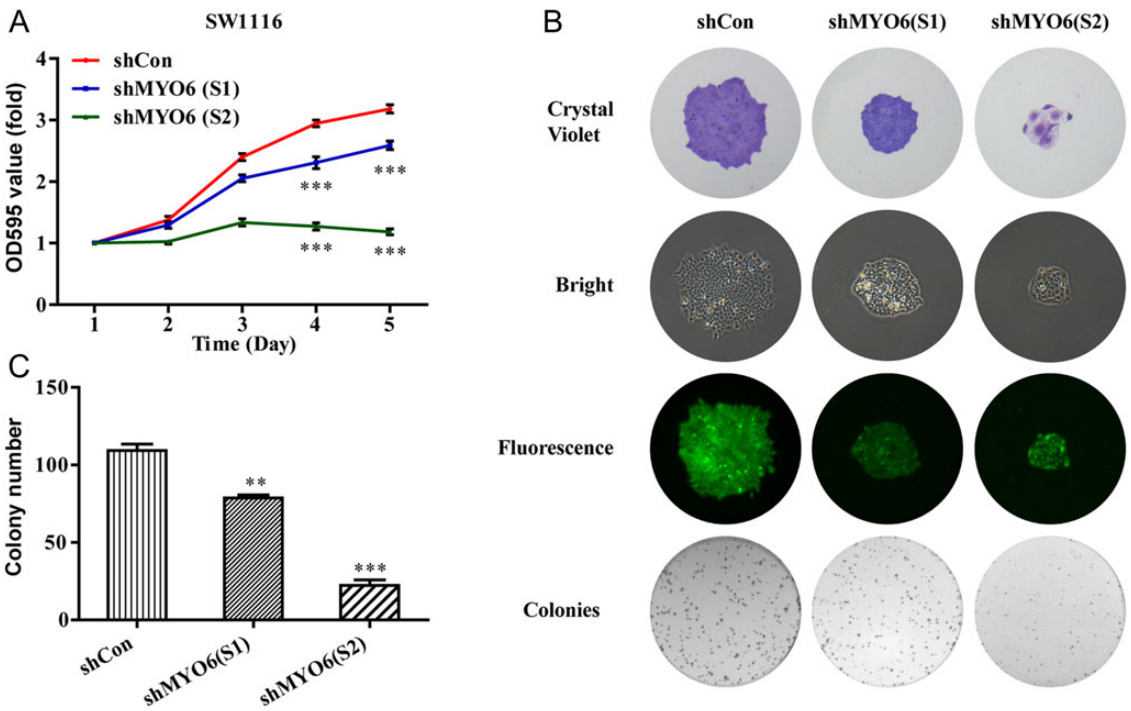

Figure 3. Knockdown of MYO6 inhibited the viability and proliferation of SW1116 cells (A) The growth curve of SW1116 cells with shCon, shMYO6(S1), or shMYO6 (S2) treatment assessed by MTT assay. (B) Images recorded under micro- and macroview, representing the size and the number of colonies in each group of cells. (C) The number of colonies formed in SW1116 cells with three different treatments. Data were presented as the mean ± SD from three independent experiments. **$P < 0.01$, ***$P < 0.001$.

assess whether *MYO6* knockdown cells really underwent apoptosis (**Fig. 5A**). As shown in **Fig. 5B**, the percentage of early apoptotic cells was increased from 5.7% to 19.6% in shMYO6(S2) group. Likewise, compared with control group shCon, the percentage of late apoptotic cells in SW1116 cells treated with shMYO6(S2) was increased from 2.1% to 24.0%. The above results suggested that the

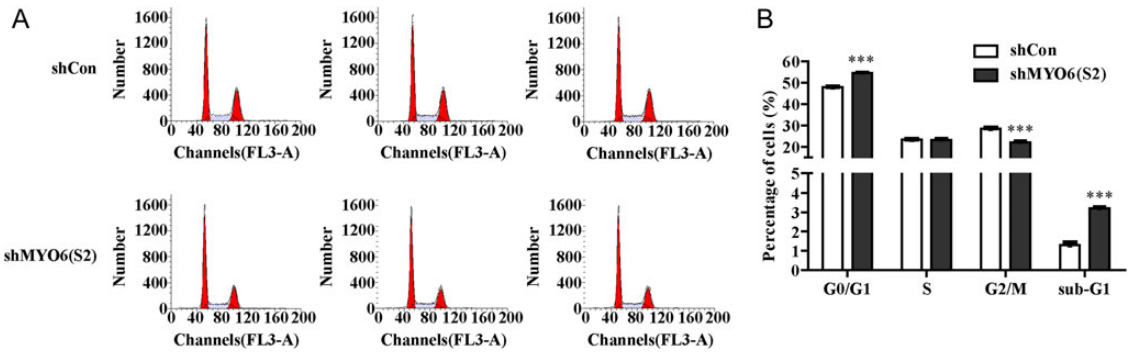

Figure 4. Knockdown of MYO6 induced cell cycle arrest in SW1116 cells (A) FACS analysis of cell cycle distribution in SW1116 cells. (B) Representative graphs of three independent experiments about the percentage of cells in different phases in SW1116 cell. Data were presented as the mean ± SD from three independent experiments. ***$P < 0.001$.

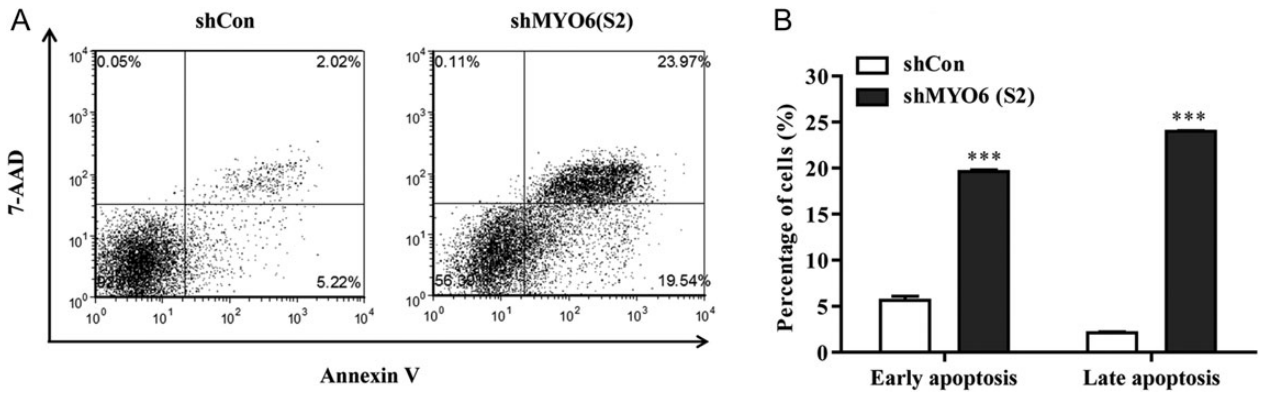

Figure 5. Knockdown of MYO6 induced cell apoptosis in SW1116 cells (A) Apoptotic cells were evaluated by Annexin V-APC/7-AAD double staining and flow cytometry in SW1116 cells following lentivirus infection in shCon group and shMYO6(S2) group. (B) Quantification of early and late apoptotic cells in SW1116 cells. ***$P < 0.001$.

inhibition of *MYO6* gene induced a strong proapoptotic effect in human CRC SW1116 cells.

Discussion

Oncomine is the biggest cancer microarray database currently available, as well as a web-based data mining platform to dig the cancer gene information [19]. In the present study, we used data mining of five independent microarray datasets (Sabates-Bellver Colon, Skrzypczak Colorectal, Hong Colorectal, Kaiser Colon, and TCGA Colorectal) in the Oncomine database and proved the overexpression of *MYO6* in CRC. The similar correlation has also been reported between *MYO6* expression and other cancers such as prostate cancer [25,26], lung adenocarcinoma [27], hepatocellular carcinoma [28], and centroblastic lymphoma [29]. In addition, Yoshida *et al.* [13] found that elevation of *MYO6* level was positively correlated with the aggressiveness of ovarian cancer both *in vitro* and *in vivo*, implying that *MYO6* plays a potential role in the carcinogenesis or malignant transformation of tumors, and is a valuable biomarker for ovarian cancer.

MYO6 plays an important role in cellular transport and anchoring, and also participates in different cellular processes such as cell endocytosis, migration, cell division, and cytokinesis. At present, most of the research results showed that high *MYO6* expression could accelerate tumor cell migration. In prostate cancer cell line LNCaP, knockdown of *MYO6* impaired cell migration and anchorage independent growth ability by regulating the expression of tumor suppressor genes TXNIP (thioredoxin-interacting protein 1), but did not affect the proliferation rate of cells in the culture medium [14]. Consistent with this, Yoshida *et al.* [13] found that silencing the *MYO6* expression could hinder the initial migration process in ovarian cancer. Likewise, *MYO6* expression was positively correlated with the expression of epithelial-mesenchymal transition markers E-cadherin and β-catenin in human renal cell carcinoma and border cells that behave like cancer cells [30,31]. However, there are few reports showing the potential biological functions of *MYO6* in tumor cell proliferation especially in CRC.

Detection of cell proliferation and apoptosis is the most common way to evaluate and measure the tumor responses to oncogenes or tumor suppressor genes. Herein, we found that knockdown of *MYO6* by small interfering RNA inhibited the growth and proliferation of CRC SW1116 cells, and also arrested cell cycle progression to some extent. Meanwhile, knockdown of *MYO6* significantly increased the proportion of sub-G1 cells and led to cell apoptosis in SW1116 cells. Sub-G1 phase cells are usually considered to be the result of apoptotic DNA fragmentation because DNA is resolved by endonucleases in cells during apoptosis [32]. Generally speaking, the DNA content in apoptotic cells is less than normal diploid cells in the nucleus, leading to a sub-G1 peak, which can be used to confirm the relative number of apoptotic cells in DNA histogram of FACS

[33,34]. Consistent with these findings, Jung *et al*. [35] demonstrated that silencing of *MYO6* could attenuate activation of p53 and impair the integrity of Golgi complex, thus enhancing the susceptibility of *MYO6*-deficient cells to DNA damage-induced apoptosis.

Collectively, this is the first study to report that *MYO6* is a novel regulator of proliferation and apoptosis in CRC. Overexpression of *MYO6* mediates tumor cell survival through enhancing cell growth and inhibiting apoptosis. Although the precise mechanism underlying the effect of *MYO6* on CRC cell proliferation and apoptosis needs to be further defined, this study provides a basic conception for recognizing novel target molecules that may control the development and progression of human CRC. Further research is required to provide more convincing evidence to support the possibility of using *MYO6* as a new and potential therapeutic target against CRC.

Funding

This work was supported by the grants from the National Natural Science Foundation of China (No. 81372311) and Shanghai Health and Family Planning Commission Research Project (No. 20134024).

References

1. Jemal A, Bray F, Center MM, Ferlay J, Ward E, Forman D. Global cancer statistics. *CA Cancer J Clin* 2011, 61: 69–90.
2. Siegel R, DeSantis C, Jemal A. Colorectal cancer statistics, 2014. *CA Cancer J Clin* 2014, 64: 104–117.
3. Jemal A, Siegel R, Ward E, Murray T, Xu J, Smigal C, Thun MJ. Cancer statistics, 2006. *CA Cancer J Clin* 2006, 56: 106–130.
4. Hong X, Chen G, Wang M, Lou C, Mao Y, Li Z, Zhang Y. STAT5a-targeting miRNA enhances chemosensitivity to cisplatin and 5-fluorouracil in human colorectal cancer cells. *Mol Med Rep* 2012, 5: 1215–1219.
5. Huh JW, Cho CK, Kim HR, Kim YJ. Impact of resection for primary colorectal cancer on outcomes in patients with synchronous colorectal liver metastases. *J Gastrointest Surg* 2010, 14: 1258–1264.
6. D'Angelica M, Kornprat P, Gonen M, DeMatteo RP, Fong Y, Blumgart LH, Jarnagin WR. Effect on outcome of recurrence patterns after hepatectomy for colorectal metastases. *Ann Surg Oncol* 2011, 18: 1096–1103.
7. Berg JS, Powell BC, Cheney RE. A millennial myosin census. *Mol Biol Cell* 2001, 12: 780–794.
8. Hartman MA, Spudich JA. The myosin superfamily at a glance. *J Cell Sci* 2012, 125: 1627–1632.
9. Wu X, Jung G, Hammer JA III. Functions of unconventional myosins. *Curr Opin Cell Biol* 2000, 12: 42–51.
10. Krendel M, Mooseker MS. Myosins: tails (and heads) of functional diversity. *Physiology* 2005, 20: 239–251.
11. Chibalina MV, Puri C, Kendrick-Jones J, Buss F. Potential roles of myosin VI in cell motility. *Biochem Soc Trans* 2009, 37: 966–970.
12. Buss F, Spudich G, Kendrick-Jones J. Myosin VI: cellular functions and motor properties. *Annu Rev Cell Dev Biol* 2004, 20: 649–676.
13. Yoshida H, Cheng W, Hung J, Montell D, Geisbrecht E, Rosen D, Liu J, *et al*. Lessons from border cell migration in the *Drosophila* ovary: a role for myosin VI in dissemination of human ovarian cancer. *Proc Natl Acad Sci USA* 2004, 101: 8144–8149.
14. Dunn TA, Chen S, Faith DA, Hicks JL, Platz EA, Chen Y, Ewing CM, *et al*. A novel role of myosin VI in human prostate cancer. *Am J Pathol* 2006, 169: 1843–1854.
15. Puri C, Chibalina MV, Arden SD, Kruppa AJ, Kendrick-Jones J, Buss F. Overexpression of myosin VI in prostate cancer cells enhances PSA and VEGF secretion, but has no effect on endocytosis. *Oncogene* 2010, 29: 188–200.
16. Wei S, Dunn TA, Isaacs WB, De Marzo AM, Luo J. GOLPH2 and MYO6: putative prostate cancer markers localized to the Golgi apparatus. *Prostate* 2008, 68: 1387–1395.
17. Bermudo R, Abia D, Mozos A, García-Cruz E, Alcaraz A, Ortiz AR, Thomson TM, *et al*. Highly sensitive molecular diagnosis of prostate cancer using surplus material washed off from biopsy needles. *Br J Cancer* 2011, 105: 1600–1607.
18. Yu H, Zhu Z, Chang J, Wang J, Shen X. Lentivirus-mediated silencing of myosin VI inhibits proliferation and cell cycle progression in human lung cancer cells. *Chem Biol Drug Des* 2015, 86: 606–613.
19. Rhodes DR, Yu J, Shanker K, Deshpande N, Varambally R, Ghosh D, Barrette T, *et al*. ONCOMINE: a cancer microarray database and integrated data-mining platform. *Neoplasia* 2004, 6: 1–6.
20. Chen YB, Lan YW, Chen LG, Huang TT, Choo KB, Cheng WT, Lee HS, *et al*. Mesenchymal stem cell-based HSP70 promoter-driven VEGFA induction by resveratrol alleviates elastase-induced emphysema in a mouse model. *Cell Stress Chaperon* 2015, 20: 979–989.
21. Sabates-Bellver J, Van der Flier LG, de Palo M, Cattaneo E, Maake C, Rehrauer H, Laczko E, *et al*. Transcriptome profile of human colorectal adenomas. *Mol Cancer Res* 2007, 5: 1263–1275.
22. Skrzypczak M, Goryca K, Rubel T, Paziewska A, Mikula M, Jarosz D, Pachlewski J, *et al*. Modeling oncogenic signaling in colon tumors by multidirectional analyses of microarray data directed for maximization of analytical reliability. *PLoS One* 2010, 5: pii: e13901.
23. Hong Y, Downey T, Eu KW, Koh PK, Cheah PY. A 'metastasis-prone' signature for early-stage mismatch-repair proficient sporadic colorectal cancer patients and its implications for possible therapeutics. *Clin Exp Metastasis* 2010, 27: 83–90.
24. Kaiser S, Park YK, Franklin JL, Halberg RB, Yu M, Jessen WJ, Freudenberg J, *et al*. Transcriptional recapitulation and subversion of embryonic colon development by mouse colon tumor models and human colon cancer. *Genome Biol* 2007, 8: R131.
25. Lapointe J, Li C, Higgins JP, van de Rijn M, Bair E, Montgomery K, Ferrari M, *et al*. Gene expression profiling identifies clinically relevant subtypes of prostate cancer. *Proc Natl Acad Sci USA* 2004, 101: 811–816.
26. Singh D, Febbo PG, Ross K, Jackson DG, Manola J, Ladd C, Tamayo P, *et al*. Gene expression correlates of clinical prostate cancer behavior. *Cancer Cell* 2002, 1: 203–209.
27. Okayama H, Kohno T, Ishii Y, Shimada Y, Shiraishi K, Iwakawa R, Furuta K, *et al*. Identification of genes upregulated in ALK-positive and EGFR/KRAS/ALK-negative lung adenocarcinomas. *Cancer Res* 2012, 72: 100–111.
28. Roessler S, Jia HL, Budhu A, Forgues M, Ye QH, Lee JS, Thorgeirsson SS, *et al*. A unique metastasis gene signature enables prediction of tumor relapse in early-stage hepatocellular carcinoma patients. *Cancer Res* 2010, 70: 10202–10212.
29. Basso K, Margolin AA, Stolovitzky G, Klein U, Dalla-Favera R, Califano A. Reverse engineering of regulatory networks in human B cells. *Nat Genet* 2005, 37: 382–390.
30. Ronkainen H, Kauppila S, Hirvikoski P, Vaarala MH. Evaluation of myosin VI, E-cadherin and beta-catenin immunostaining in renal cell carcinoma. *J Exp Clin Cancer Res* 2010, 29: 2.
31. Geisbrecht ER, Montell DJ. Myosin VI is required for E-cadherin-mediated border cell migration. *Nat Cell Biol* 2002, 4: 616–620.
32. Zhang YF, Jiang R, Li JD, Zhang XY, Zhao P, He M, Zhang HZ, *et al*. SMC1A knockdown induces growth suppression of human lung adenocarcinoma cells through G1/S cell cycle phase arrest and apoptosis pathways *in vitro*. *Oncol Lett* 2013, 5: 749–755.
33. Riccardi C, Nicoletti I. Analysis of apoptosis by propidium iodide staining and flow cytometry. *Nat Protocol* 2006, 1: 1458–1461.
34. Elstein KH, Zucker RM. Comparison of cellular and nuclear flow cytometric techniques for discriminating apoptotic subpopulations. *Exp Cell Res* 1994, 211: 322–331.
35. Jung EJ, Liu G, Zhou W, Chen X. Myosin VI is a mediator of the p53-dependent cell survival pathway. *Mol Cell Biol* 2006, 26: 2175–2186.